Received December 3, 2019, accepted January 27, 2020, date of publication February 6, 2020, date of current version February 17, 2020.

Digital Object Identifier 10.1109/ACCESS.2020.2972160

A New Class of Dual-Band Waveguide Filters Based on Chebyshev Polynomials of the Second Kind

YUHAO LEONG, SOVUTHY CHEAB, (Member, IEEE), SOCHEATRA SOEUNG, (Member, IEEE), AND PENG WEN WONG, (Senior Member, IEEE)

Department of Electrical and Electronic Engineering, Petronas University of Technology, Tronoh 32610, Malaysia

Corresponding author: Socheatra Soeung (socheatra.s@utp.edu.my).

This work was supported by the Yayasan Universiti Teknologi PETRONAS (YUTP-FRG) under Grant 015LC0-093.

ABSTRACT This paper presents for the first time a method of mathematical synthesis involving chaining of Chebyshev polynomials of the second kind for the application of a dual-band waveguide filter. This method takes advantage of second kind Chebyshev polynomials that have high out-of-band rejection, and overcomes unequal-ripple properties. It is applicable to high filter orders greater than five, and will always possess symmetrical dual-band filter properties. This proposed approach is able to achieve an optimum and constant ripple, the flexibility of return loss, and high adjacent band's rejection. The design method is based on suitably defined transmission zeros at the centred frequency to the chained Chebyshev of the second kind. A sixth-order waveguide filter based on a prescribed return loss of 15 dB centred at a frequency of 28 GHz, with a fractional bandwidth of 1% in each passband, has been implemented and fabricated. The measured results show that the return loss, total bandwidth, and the frequency shift are 12 dB, 860 MHz, and 0.24%, respectively. The measured and ideal responses of the waveguide model are in a good agreement.

INDEX TERMS Narrowband, second kind Chebyshev, symmetrical dual-bandpass filters, transmission zeros, waveguide.

I. INTRODUCTION

Since modern communication uses complex frequency channels, dual-band and multi-band filters have a crucial role in simplifying the system and reducing the mass and volume of the circuit. In recent years, filtering characteristics with more than one passband have been finding applications in microwave telecommunication systems. Incorporating two passbands within a single filter structure offers advantages over the equivalent 'dual-diplexer' solution in terms of mass per volume and ease of manufacturing and tuning [1], [2]. Four approaches are usually employed to implement multi-band filters: (i) broadband bandpass and bandstop filter cascading [3]; (ii) the use of multiple harmonic resonating modes of resonators [4]; (iii) the use of parallel-connected filter [5]; and (iv) single filter structure realisation with transmission zero [2], [6].

The associate editor coordinating the review of this manuscript and approving it for publication was Jenny Mahoney.

A. BROADBAND BANDPASS AND BANDSTOP FILTER CASCADING

A dual-band filter consists of a bandstop filter and a wide-band bandpass filter in a cascade connection. The bandstop and the wide-band bandpass filters are implemented using equal-length serial-shunted line configurations [3].

Using this method for dual-band bandpass filter design, a minimum insertion loss can be obtained due to the Butterworth properties, which can reduce the Chebyshev insertion loss. However, in order to synthesise the dual-band bandpass filter, the Chebyshev filter has to be cascaded with the Butterworth filter [3]. As a result, more components will be involved, and the size of the filter will be increased.

B. MULTIPLE HARMONIC RESONATING MODES OF RESONATORS

This method introduces a coupling structure with transmission-line resonators coupled at the ends and the centre to yield tunable dual-band couplings [4]. This is designed to overcome the difficulty of finding the desired coupling coefficients at both fundamental resonant frequencies f_1 and f_2 with different electric fields, magnetic fields and electrical coupling properties.

The advantage of this method is the tuning flexibility of the dual-band couplings, which utilises the properties of the electric and magnetic fields to introduce the transmission zeros at the passbands. However, it needs the dual-band matching network in order to achieve the dual-band loaded Qs, meaning that extra components are needed that cause the filters to be larger in size [4].

C. THE USE OF PARALLEL-CONNECTED FILTER

A dual-band filter is constituted by two sub-networks connected in parallel, which are obtained from suitable transformations of the lowpass transversal canonical prototype [5]. It is designed to allow a large separation of the two passbands and the ease in tuning.

The advantage of this method is that it allows the practical feasibility of dual-band filters especially for the case of needing a large separation of the two passbands, with the help of having shunt connections of two passbands sub-networks that can each operates as a single passband. However, it needs the input nodes and two-passband sub-networks to achieve dual-band filters. As a result, extra components are needed that cause the filters to be larger in size [5].

D. SINGLE FILTER STRUCTURE REALISATION WITH TRANSMISSION ZEROS IN THE PASSBAND

Transmission zeros produced by cross-coupling or bandstop resonators are used to split a single passband into dual passbands or multiple passbands based on a single filter circuit [2], [6], [7]. In this topology, a bandpass resonator and all the bandstop resonators that are properly coupled to this bandpass resonator comprise of the inverter coupled-resonator sections.

The advantage of using inverter coupled-resonator sections is that it allows realising a single filter structure with transmission zeros without extra components, such as the two cascading filters and the dual-band matching network. In addition, this configuration is able to generate the same in-band and out-of-band responses for every band [8]. However, the complexity of the filter will be increased for an extremely narrow band with high order filter design.

E. CHEBYSHEV FILTERS

The specifications of modern filter design require smaller fractional bandwidths, higher frequencies of operation, lower manufacturing costs and shorter development times. Most of the microwave and millimetre-wave bandpass filters that are currently manufactured are of the Chebyshev family. Chebyshev filters have equal-ripple passbands with steeper roll-off than Butterworth filters. The generalised expression for the Chebyshev filtering function is shown below:

$$T_N(\omega) = \cosh \sum_{n=1}^{\infty} \cosh^{-1} x_n(\omega) \tag{1}$$

where $x_n(\omega)$ is the function of the frequency variable ω.

The Chebyshev class of filtering function has the generic features of equal-ripple amplitude in-band characteristics, together with the sharpest cut-off at the edge of the passband and high selectivity, giving an acceptable compromise between the lowest signal degradation and highest noise/interference rejection [9]. However, narrow-band high-order conventional Chebyshev filters will have their reflection coefficient zeros distributed over an extremely small frequency range and require a post-manufacturing tuning process, due to the limitations of fabrication technology in terms of delivering the actual filter design parameters [10].

One solution to these problems is the implementation of a chained function in the design of the filter, which maximises the benefits of reduced sensitivity to manufacturing errors. The chained function can produce a variety of transfer functions based on pre-defined manufacturing limitations [10]. The method in this paper can be divided into three steps:

(i) Generating chained-function expressions based on Chebyshev characteristic functions of the second kind;

(ii) Generating the chained-function ripple factor expressions;

(iii) Generating the symmetrical dual-band chained- function expressions.

F. CHAINED-FUNCTION FILTERS

Chained functions can be considered in terms of a compromise between the Butterworth and Chebyshev approximations. They contain a ''Seed Function'' and can form a bridge between the low sensitivity, low resonator unloaded-Q, low loss filter properties of the Butterworth approximations and the high out-of-band rejection properties of the conventional Chebyshev filters [10]. The key advantage of the chained function is that it allows the designer to use this function as a seed function and to chain with itself until the right out-of-band rejection is achieved. This effectively means that multiple reflection zeros can be placed at the same frequency. The resulting chained function has been proven in [11], [12] to have reduced sensitivity to manufacturing errors while maintaining a rejection performance that is comparable to conventional Chebyshev filters even in the case of using a low-accuracy microstrip fabrication process. The transfer function of the chained function (CF) can be expressed in terms of the CF filtering function, $C_N(\omega)$ and the CF ripple factor, ε_c [9]:

$$|S_{21}(\omega)|^2 = \frac{1}{1+\varepsilon_C^2 C_N(\omega)^2} \tag{2}$$

II. THEORY OF SYMMETRICAL DUAL PASSBAND PROTOTYPES

A. CHEBYSHEV POLYNOMIALS OF THE SECOND KIND

Fig. 1 shows the characteristics of the sixth-degree conventional Chebyshev and Chebyshev of the second kind polynomials. It can be observed that the conventional Chebyshev demonstrates equal-ripple behaviours while the second kind

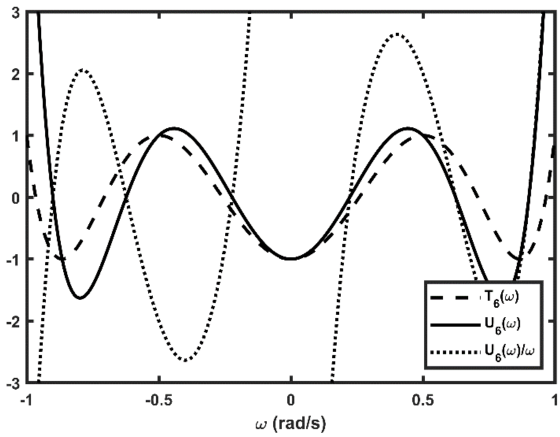

FIGURE 1. Comparison of sixth-degree conventional Chebyshev, $T_6(\omega)$ and Chebyshev of the second kind, $U_6(\omega)$ together with Chebyshev of the second kind with a transmission zero, TZ at the zero frequency.

does not. However, after introducing a TZ to the second kind Chebyshev filtering function, the ripple levels nearer to the TZ position are higher than those closer to the out-of-band rejection. As a result, it is possible to suitably introduce TZs to the respective filter order so that the equal-ripple behaviour can be reinstalled. Hence, the second kind Chebyshev filtering functions are used in the design of the dual-band filter. The second kind Chebyshev characteristic function, U_N is defined as:

$$U_N = \frac{\sinh[(N+1)\theta]}{\sinh\theta} \quad (3)$$

where N is the number of filter order. By substituting $\omega = \cosh\theta$, $U_N(\omega)$ can be written as:

$$U_N(\omega) = \frac{\sinh(\sum_{1}^{N+1} \cosh^{-1}\omega)}{\sinh(\cosh^{-1}\omega)} \quad (4)$$

By replacing the $\cosh^{-1}$ term in (4) with Euler's identity, the characteristic function, $U_N(\omega)$ can be rewritten in exponential form:

$$U_N(\omega) = \frac{\prod_{1}^{N+1} X - \prod_{1}^{N+1} \frac{1}{X}}{X - \frac{1}{X}} \quad (5)$$

where $X = ln(\omega + \sqrt{\omega^2 - 1})$.

B. CHAINED FUNCTION BASED ON CHEBYSHEV OF THE SECOND KIND

Table 1 shows the sixth-degree chained-function polynomials based on Chebyshev polynomials of the second kind for different seed function orders. The combination of seed function orders (2, 4) was chosen as it has six distinct poles that can clearly depict the passband equal-ripple behaviour after introducing TZs at $\omega = 0$ rad/s. Similar seed function orders are implemented for the eighth- and tenth-order chained function polynomials by subsequently adding a seed function of order two. By chaining the seed function orders (2, 4), (2, 2, 4), and (2, 2, 2, 4), the comparisons between different filter orders of second kind Chebyshev and chained-function responses based on $U_N(\omega)$ are illustrated in Figs. 2 (a) – (c).

TABLE 1. Chained-function polynomials for $N_T = 6$.

No. of Seed Functions	Orders of the Seed Functions	Chained Function Polynomials
6	1, 1, 1, 1, 1, 1	$64\omega^6$
5	1, 1, 1, 1, 2	$64\omega^6 - 16\omega^4$
4	1, 1, 2, 2	$64\omega^6 - 32\omega^4 + 4\omega^2$
4	1, 1, 1, 3	$64\omega^6 - 32\omega^4$
3	1, 2, 3	$64\omega^6 - 48\omega^4 + 8\omega^2$
3	1, 1, 4	$64\omega^6 - 48\omega^4 + 4\omega^2$
3	2, 2, 2	$64\omega^6 - 48\omega^4 + 12\omega^2 - 1$
2	3, 3	$64\omega^6 - 64\omega^4 + 16\omega^2$
2	2, 4	$64\omega^6 - 64\omega^4 + 16\omega^2 - 1$
2	1, 5	$64\omega^6 - 64\omega^4 + 12\omega^2$
1	6	$64\omega^6 - 80\omega^4 + 24\omega^2 - 1$

Both second kind Chebyshev and chained-function responses depict similar selectivity. In other words, rejection properties of the second kind Chebyshev characteristic functions were not sacrificed using chained-function characteristic functions. This shows that the chained function for seed function order (2, 4) only distorts the ripple levels. In addition, the poles for the higher-order chained function will not be distributed over an extremely small frequency range, since the number of distinct poles will always be a constant at six due to the properties of the chained function, thus reducing the effort involved in the post-manufacturing tuning process compared to Chebyshev filters [12]. The resultant responses, which always have a constant six distinct poles for the higher-order chained functions, facilitate the modelling of the dual-band chained-function filter after introducing TZs at $\omega = 0$ rad/s. Thus, chained functions with seed function order (2^n, 4) are considered for the dual-band waveguide filter design.

C. NUMBER OF TRANSMISSION ZEROS (TZS) TO BE INTRODUCED

To implement the single filter structure with TZs to the chained functions, the sixth-order chained function based on the seed function order (2, 4) is chosen. In addition, by introducing TZs at $\omega = 0$ rad/s to the chained function, the passband equal-ripple behaviours can be reinstalled. In order to determine the number of TZs needed to realise the symmetrical sixth-order dual-band chained-function filter with passband equal-ripple behaviours, several TZs have been introduced at $\omega = 0$ rad/s, as shown in Fig. 3.

The lower band-edge of the lowest frequency band and the upper band-edge of the highest frequency band are always fixed at $\omega = -1$ rad/s and $\omega = +1$ rad/s, respectively. By introducing four and five TZs to the eighth- and tenth-order chained functions, based on seed function orders (2^n, 4), symmetrical dual-band filter responses with passband equal-ripple behaviours are obtained, as shown in Fig. 4.

Thus, in order to achieve symmetrical dual-band chained functions with passband equal-ripple behaviours, the number of TZs to be introduced at $\omega = 0$ rad/s to the chained

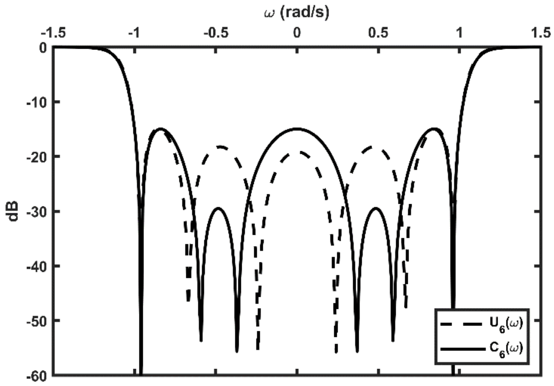

(a) U_6 and C_6

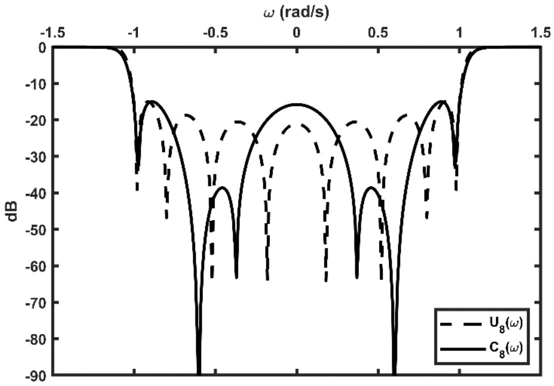

(b) U_8 and C_8

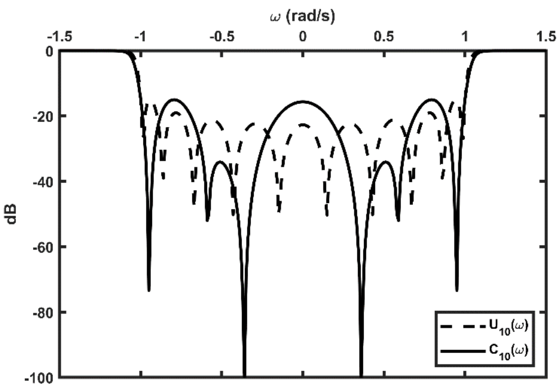

(c) U_{10} and C_{10}

FIGURE 2. Comparison between the second kind Chebyshev and chained-function responses in terms of S_{11}.

functions with seed function order (2^n, 4) can be deduced as:

$$\alpha = \frac{\beta}{2} \tag{6}$$

where α is the number of TZs to be introduced and β is the filter order of the chained function based on seed function order (2^n, 4).

D. GENERAL EXPRESSION FOR THE CHAINED FUNCTION POLYNOMIALS OF THE SECOND KIND

A sixth-order chained function, $C_6(\omega)$ can be obtained by chaining a seed function order (2, 4) of the second kind

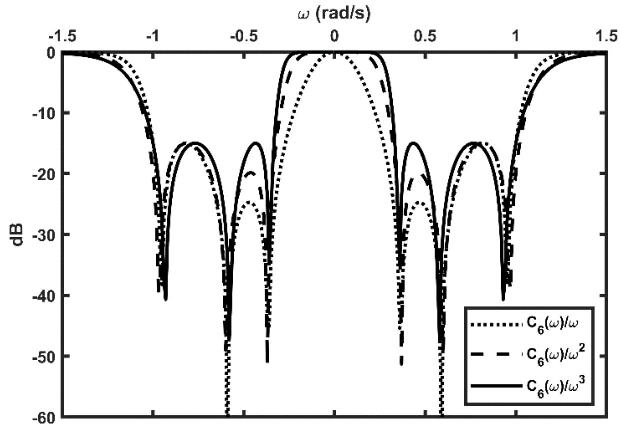

FIGURE 3. Comparison between sixth-order dual-band chained-function responses with seed function order (2, 4) and different TZs in terms of S_{11}. Three TZs have to be introduced at $\omega = 0$ rad/s to achieve the passband equal-ripple behaviour.

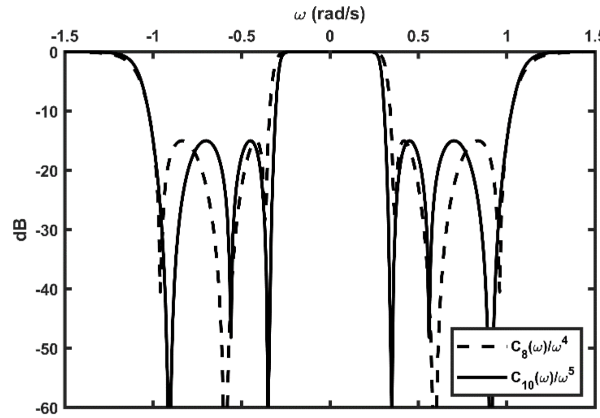

FIGURE 4. Symmetrical eighth- and tenth-order dual-band chained-function responses with seed function order (2^n, 4) and different TZs introduced in terms of S_{11}.

Chebyshev characteristic functions, $U_2(\omega)$ and $U_4(\omega)$:

$$C_6(\omega) = \frac{Y^3 - 1}{Y(Y-1)} \times \frac{Y^5 - 1}{Y^2(Y-1)} \tag{7}$$

where $Y = ln(\omega + \sqrt{\omega^2 - 1})$.

Using the partial fraction, $C_6(\omega)$ becomes:

$$C_6(\omega) = \frac{Y^3 - 1}{Y(Y-1)} + \frac{Y^5 - 1}{Y^2(Y-1)} + \frac{Y^7 - 1}{Y^3(Y-1)} \tag{8}$$

or

$$C_6(\omega) = \sum_{k=1}^{3} \frac{Y^{2k+1} - 1}{Y^k(Y-1)} \tag{9}$$

The eighth-order chained function, $C_8(\omega)$ is obtained by chaining $C_6(\omega)$ and $U_2(\omega)$:

$$C_8(\omega) = C_6(\omega) \times U_2(\omega) \tag{10}$$

By using partial fraction and the expression of $C_6(\omega)$ from (9), $C_8(\omega)$ can be expressed as:

$$C_8(\omega) = \sum_{i=1}^{3} \sum_{k=|i-1|}^{i+1} \frac{Y^{2k+1}-1}{Y^k(Y-1)} \tag{11}$$

Generally, the higher-order chained functions, $C_N(\omega)$ of degree $N \geq 6$, can be expressed using the recursive formula as:

$$C_N(\omega) = C_{N-2}(\omega) \times U_2(\omega) \tag{12}$$

It should be mentioned that $N = 2^n + 4$ where n is an integer. To find $C_N(\omega)$ using (12), it is useful to use the developed general expression for the multiplication of Chebyshev polynomials of orders i and j ($U_i(\omega)$ and $U_j(\omega)$):

$$U_i(\omega) \times U_j(\omega) = \sum_{k=\frac{|i-j|}{2}}^{\frac{i+j}{2}} \frac{Y^{2k+1}-1}{Y^k(Y-1)} \tag{13}$$

E. RIPPLE FACTOR OF THE GENERALISED CHAINED FUNCTIONS

Following [13], the transfer function (S_{21}) for the Chebyshev filtering functions is:

$$|S_{21}(\omega)|^2 = \frac{1}{1+\varepsilon^2 \times |FF(\omega)|^2} \tag{14}$$

where ε is the ripple factor for the Chebyshev filtering functions and $FF(\omega)$ is the Chebyshev filtering functions. When $|FF(\omega)|$ is at maximum, e.g. $|FF(\omega)| = 1$, the transfer function for the chained function can be deduced by multiplying (14) with $FF_C(\omega)$:

$$|S_{21}(\omega)|^2 = \frac{1}{1+[\frac{\varepsilon}{FF_c(\omega)}]^2 \times |FF_C(\omega)|^2} \tag{15}$$

where $FF_C(\omega)$ is the chained-function filtering functions which oscillate between -1 rad/s and $+1$ rad/s. When $|FF_C(\omega)|$ is at maximum, e.g. $|FF_C(\omega)| = 1$, by substituting the ripple factor of the Chebyshev filtering function, $\varepsilon = \frac{1}{\sqrt{10^{\frac{RL}{10}}-1}}$, the generalised passband ripple factor for chained-function filtering functions ε_C can be derived as:

$$\varepsilon_C = \frac{1}{\sqrt{10^{\frac{RL_C}{10}}-1} \times |FF_C|} \tag{16}$$

where RL_C is the prescribed chained-function return loss in dB.

F. GENERALISED SYMMETRICAL DUAL-BAND CHAINED FUNCTIONS

The generalised Chebyshev transfer function, S_{21} and reflection function, S_{11} are expressed [13]:

$$|S_{11}(\omega)|^2 = 1 - \frac{1}{1+\varepsilon^2 \times |FF(\omega)|^2} \tag{17}$$

$$|S_{21}(\omega)|^2 = \frac{1}{1+\varepsilon^2 \times |FF(\omega)|^2} \tag{18}$$

where ε is the prescribed Chebyshev ripple factor and $FF(\omega)$ is the Chebyshev filtering function.

Using (6), (12) and (16), the generalised symmetrical dual-band chained function based on seed function order (2^n, 4) with TZs at $\omega = 0$ for S_{11} and S_{21} can be derived as:

$$|S_{11}(\omega)|^2 = 1 - \frac{1}{1+\varepsilon_C^2 \times |\frac{C_N(\omega)}{\omega^\alpha}|^2} \tag{19}$$

$$|S_{21}(\omega)|^2 = \frac{1}{1+\varepsilon_C^2 \times |\frac{C_N(\omega)}{\omega^\alpha}|^2} \tag{20}$$

where ε_C is the prescribed chained-function ripple factor and α is the number of TZs to be introduced.

G. PASSBAND EQUAL-RIPPLE RESPONSES

The chained-function filtering function for different filter orders with TZs can be extracted from (19) and (20) as:

$$FF_C(\omega) = \frac{C_N(\omega)}{\omega^\alpha} \tag{21}$$

In order to prescribe the return loss, $FF_c(\omega)$ has to be differentiated to determine the ω_{worst} location of the worst return loss:

$$\frac{\partial FF_C(\omega)}{\partial \omega} = 0 \tag{22}$$

The ω_{worst} location of the worst return loss found in (22) has been altered to the prescribed return loss value by using (16). In order to normalise the frequency responses, the cut-off frequencies have to be determined:

$$\begin{aligned} FF_C(\omega_{worst}) &= FF_{C(\max)} \\ &= FF_{C(cut\_off)} \end{aligned} \tag{23}$$

After normalising the frequency responses, passband equal-ripple responses have been achieved. In order to verify the passband equal-ripple responses, ω_{new} locations of the return losses can be found using (22) and substituted to (19).

III. HARDWARE REALISATION AND EXAMPLES

A. SIXTH-ORDER DUAL-BAND CHAINED-FUNCTION WAVEGUIDE FILTER

The above theory is now implemented to the sixth-order dual-band waveguide filter WR-34 with a prescribed return loss of 15 dB centred at frequency of 28 GHz and a cut-off frequency at 17.357 GHz, with a fractional bandwidth of 1% in each passband to depict the narrow band. The sixth-order chained function based on the seed function order (2, 4) of second kind Chebyshev polynomials can be expressed by using (12):

$$C_{2,4}(\omega) = 64\omega^6 - 64\omega^4 + 16\omega^2 - 1 \tag{24}$$

In order to design a sixth-order symmetrical dual-band chained function, TZs have to be introduced at zero frequency ($\omega = 0$ rad/s). The number of TZs between the two bands and the ripple factor are 3 and 0.0587, respectively, using (6) and (16). The final coupling matrix for the sixth-order dual-band chained-function waveguide filter is:

$$\begin{bmatrix} 0 & 0.823 & 0 & 0 & 0 & 0 \\ 0.823 & 0 & 0.411 & 0 & 0 & -0.418 \\ 0 & 0.411 & 0 & -0.330 & -0.235 & 0 \\ 0 & 0 & -0.330 & 0 & 0 & 0 \\ 0 & 0 & -0.235 & 0 & 0 & 0.709 \\ 0 & -0.418 & 0 & 0 & 0.709 & 0 \end{bmatrix}$$
$$Q_{C1} = Q_{C6} = 167.879 \tag{25}$$

The corresponding coupling/routing diagram is shown in Fig. 5, where each node represents a unit capacitance and the lines are admittance inverters (coupling coefficients). The solid lines represent main couplings and the dotted lines represent cross-couplings. S and L represent the source and the load, respectively. The filter topology is implemented in a waveguide filter whose 3D layout model is shown in Fig. 6 using Ansys HFSS. After running several optimisations, the final physical dimensions are listed in Table 2.

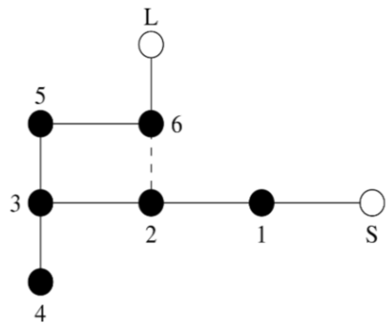

FIGURE 5. Sixth-order dual-band chained-function waveguide filter topology.

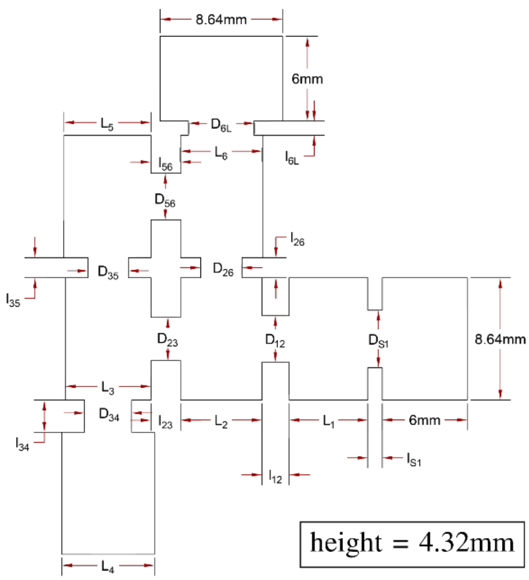

FIGURE 6. Sixth-order dual-band chained-function waveguide filter (top view).

TABLE 2. Final dimensions of the sixth-order waveguide filter.

Symbol	Value (mm)	Symbol	Value (mm)
L_1	5.56	D_{26}	2.908
L_2	5.753	D_{56}	3.2825
L_3	6.042	D_{6L}	4.632
L_4	6.54	I_{S1}	1.013
L_5	6.147	I_{12}	1.916
L_6	5.795	I_{23}	2.095
D_{S1}	4.067	I_{34}	2.265
D_{12}	3.3085	I_{35}	1.43
D_{23}	3.059	I_{26}	1.43
D_{34}	3.325	I_{56}	2.095
D_{35}	2.857	I_{6L}	1.013

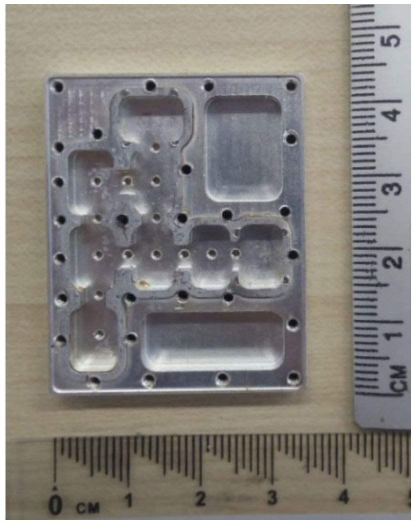

(a) Cavity without cover

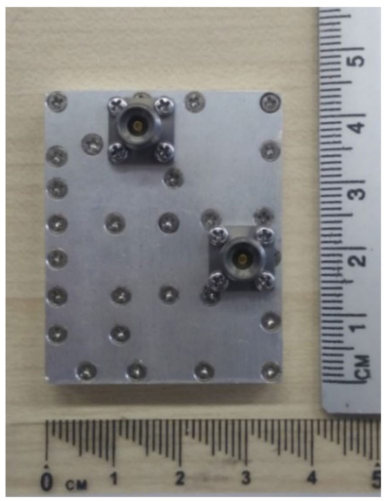

(b) Cover with the SMA connectors

FIGURE 7. Fabricated sixth-order dual-band chained-function waveguide filter.

Figs. 7 (a) – (b) present photographs of the fabricated filter without tuning screws. The realisation of the negative (capacitive) coupling and the input/output coupling through taps to the first and last resonator are shown.

The simulated sixth-order dual-band chained-function waveguide S-parameter responses are plotted in Fig. 8

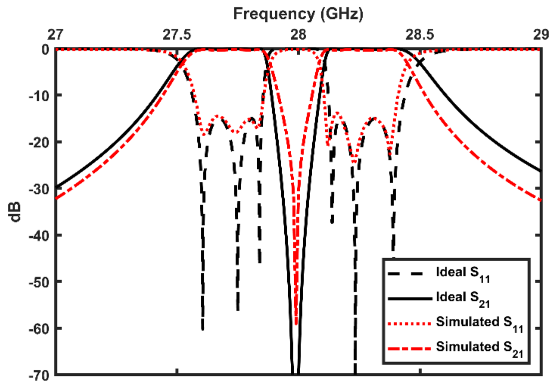

FIGURE 8. Comparison between the simulated and the ideal sixth-order dual-band chained-function waveguide S-parameters.

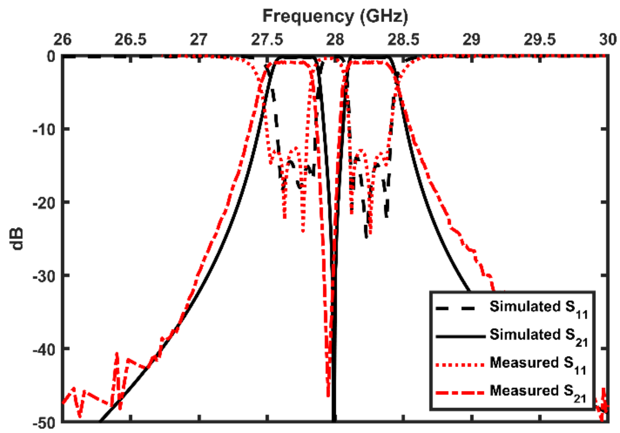

FIGURE 9. Comparison between the measured and the simulated responses of the sixth-order dual-band chained-function waveguide filter.

together with the ideal responses. The simulated results show an in-band return loss performance of 14 dB, which is comparable to the ideal return loss of 15 dB for both bands. The three TZs, total bandwidth and insertion loss in the simulation are 27.99 GHz, 810 MHz, and 0.85 dB, respectively. In addition, the simulation shows that the lower and upper bands are centred at 27.715 GHz and 28.275 GHz, respectively. The simulated and ideal responses of the sixth-order dual-band chained-function waveguide model are in a good agreement.

A comparison between simulated and measured responses is shown in Fig. 9. Centre frequencies of the filter for the lower band and the upper bands are 27.65 GHz and 28.25 GHz, respectively. The measured return loss is better than 12 dB for both passbands. The measured insertion loss of 0.93 dB is slightly higher than the simulated 0.85 dB. The total measured bandwidth of 3.07% is very close to the simulated bandwidth of 2.89%. It can be observed that there is a frequency shift of only 0.24%. The discrepancy of frequency shift is lower when realizing the filter with filter order greater than nine based on the mathematical syntheses as shown in Table 4.

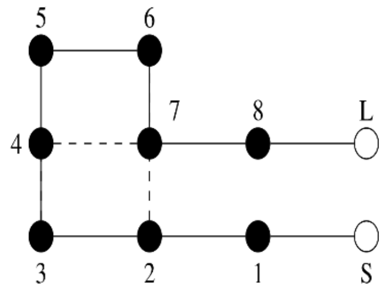

FIGURE 10. Eighth-order dual-band chained-function waveguide filter topology.

B. EIGHTH-ORDER DUAL-BAND CHAINED-FUNCTION WAVEGUIDE FILTER

To further validate the above theory for the higher filter order applications, an eighth-order dual-band chained-function is implemented in the similar WR-34 waveguide filter with a prescribed return loss of 15 dB centred at a frequency of 28 GHz to indicate the high frequency applications, and a fractional bandwidth of 0.65% in each passband to depict the narrow band.

Using (12) and (24), the eighth-order chained function based on the seed function order (2, 2, 4) can be rewritten as:

$$C_{2,2,4}(\omega) = 256\omega^8 - 320\omega^6 + 128\omega^4 - 20\omega^2 + 1 \qquad (26)$$

The number of TZs between the two bands and the ripple factors are 4 and 0.0452, respectively, using (6) and (16). The final coupling matrix for the eighth-order dual-band chained-function waveguide filter can be found as shown in (27), as shown at the bottom of the next page.

The corresponding coupling/routing diagram is shown in Fig. 10, where each node represents a unit capacitance and the lines are admittance inverters (coupling coefficients). The solid lines represent main couplings and the dotted lines represent cross-couplings. S and L represent the source and the load, respectively. The filter topology is implemented in a waveguide filter whose 3D layout model is shown in Fig. 11 using Ansys HFSS. After running several optimisations, the final physical dimensions are listed in Table 3.

TABLE 3. Final dimensions of the eighth-order waveguide filter.

Symbol	Value (mm)	Symbol	Value (mm)
L_1	5.705	D_{78}	2.84
L_2	5.985	D_{47}	2.32
L_3	6.35	D_{27}	2.66
L_4	6.135	D_{8L}	3.585
L_5	6.09	I_{S1}	1
L_6	6.48	I_{12}	1.7
L_7	5.98	I_{23}	1.35
L_8	5.88	I_{34}	1.99
D_{S1}	4.06	I_{45}	3.1
D_{12}	3.255	I_{56}	1.35
D_{23}	2.65	I_{67}	3.1
D_{34}	2.99	I_{78}	1.7
D_{45}	3.71	I_{47}	1.35
D_{56}	3.54	I_{27}	1.99
D_{67}	2.71	I_{8L}	1

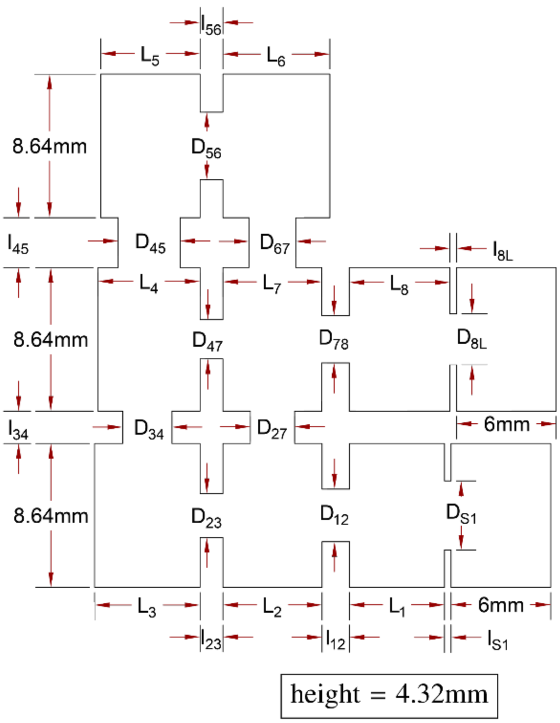

FIGURE 11. Eighth-order dual-band chained-function waveguide filter (top view).

The simulated eighth-order dual-band chained-function waveguide S-parameter responses are plotted in Fig. 12 together with the ideal responses. The simulated results show an in-band return loss performance of 13.5 dB, which is comparable with the ideal return loss of 15 dB for both bands. The three TZs, total bandwidth and insertion loss in the simulation are 27.99 GHz, 510 MHz, and 0.89 dB, respectively. In addition, the simulation shows that the lower and upper bands are centred at 27.81 GHz and 28.185 GHz, respectively. The simulated and ideal responses of eighth-order dual-band chained-function waveguide model are in a good agreement.

IV. SENSITIVITY TO MANUFACTURING ERRORS

To evaluate the sensitivity to manufacturing errors of the chained-function waveguide filter, sixth-, eighth-, tenth-, twelfth-, and fourteenth-order chained-function waveguide

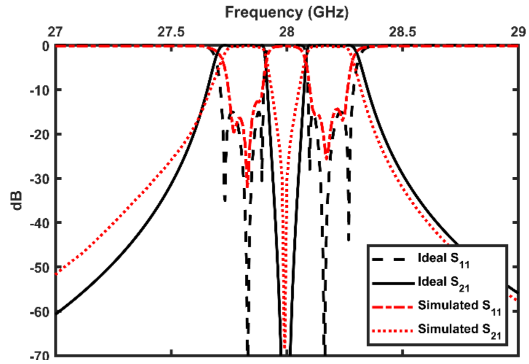

FIGURE 12. Comparison between the simulated and the ideal eighth-order dual-band chained-function waveguide S-parameters.

filters are compared with its respective filter order responses of conventional Chebyshev and Chebyshev of the second kind waveguide filters shown in Fig. 13. The sensitivity analysis is conducted by applying a ±10% tolerance to their coupling matrices and compared their filter performances to those of the ideal models [14], [15]. It should be noted that [14] and [15] are only limited to single-band filter realisations. To have a fair comparison, the worst-case passband return loss level is prescribed to 15 dB before distortion for filter responses of chained functions, conventional Chebyshev, and Chebyshev of the second kind.

Fig. 13 depicts the effects of tolerance towards the S-parameters responses for the chained functions, conventional Chebyshev, and Chebyshev of the second kind. The percentage differences in their return loss levels, insertion loss levels, and bandwidths are summarized in Table 4. Rejection levels of these filters are also summarised in Table 5 and Table 6. It should be noticed that the rejection levels for sixth-order filters are taken at frequencies of 27.2 GHz and 28.8 GHz, which are different from other filters that are taken at frequencies of 27.5 GHz and 28.5 GHz. It is because sixth- order filters have 1% larger total bandwidth than other filters. From Table 4, sixth- and eighth-order chained-function responses have 1.67% and 2.47% higher percentage changes of return losses, 4.55% and 4.54% higher percentage changes of insertion loss, together with 4.76% and 1.78% higher percentage changes of bandwidths,

$$\begin{bmatrix} 0 & 0.81 & 0 & 0 & 0 & 0 & 0 & 0 & 0 & 0 \\ 0.81 & 0 & 0.801 & 0 & 0 & 0 & 0 & 0 & 0 & 0 \\ 0 & 0.801 & 0 & 0.456 & 0 & 0 & 0 & -0.202 & 0 & 0 \\ 0 & 0 & 0.456 & 0 & -0.543 & 0 & 0 & 0 & 0 & 0 \\ 0 & 0 & 0 & -0.543 & 0 & -0.149 & 0 & 0.359 & 0 & 0 \\ 0 & 0 & 0 & 0 & -0.149 & 0 & 0.352 & 0 & 0 & 0 \\ 0 & 0 & 0 & 0 & 0 & 0.352 & 0 & -0.281 & 0 & 0 \\ 0 & 0 & -0.202 & 0 & 0.359 & 0 & -0.281 & 0 & 0.801 & 0 \\ 0 & 0 & 0 & 0 & 0 & 0 & 0 & 0.801 & 0 & 0.81 \\ 0 & 0 & 0 & 0 & 0 & 0 & 0 & 0 & 0.81 & 0 \end{bmatrix} \tag{27}$$

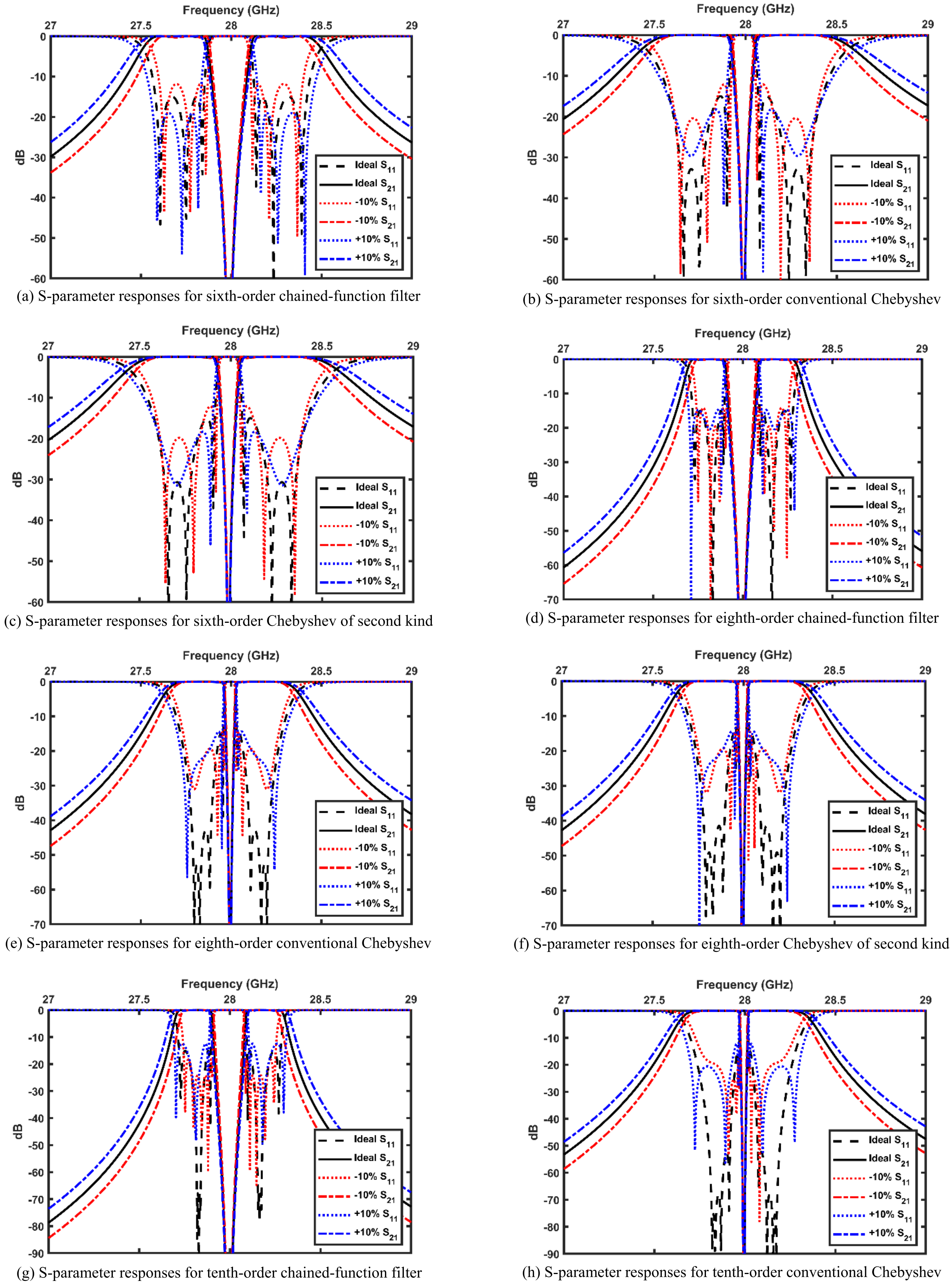

(a) S-parameter responses for sixth-order chained-function filter

(b) S-parameter responses for sixth-order conventional Chebyshev

(c) S-parameter responses for sixth-order Chebyshev of second kind

(d) S-parameter responses for eighth-order chained-function filter

(e) S-parameter responses for eighth-order conventional Chebyshev

(f) S-parameter responses for eighth-order Chebyshev of second kind

(g) S-parameter responses for tenth-order chained-function filter

(h) S-parameter responses for tenth-order conventional Chebyshev

FIGURE 13. The effect of tolerance towards the S-parameter responses for chained-function, conventional Chebyshev, and Chebyshev of the second kind for filter order of six, eight, ten, twelve, and fourteen.

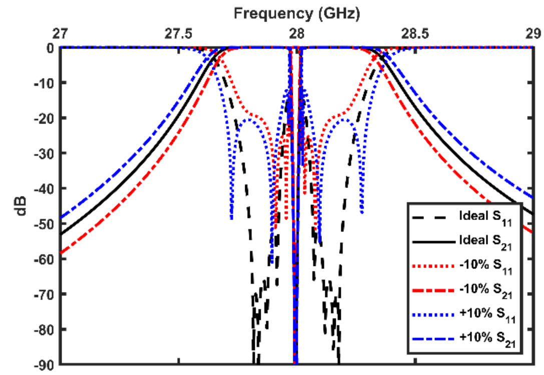

(i) S-parameter responses for tenth-order Chebyshev of second kind

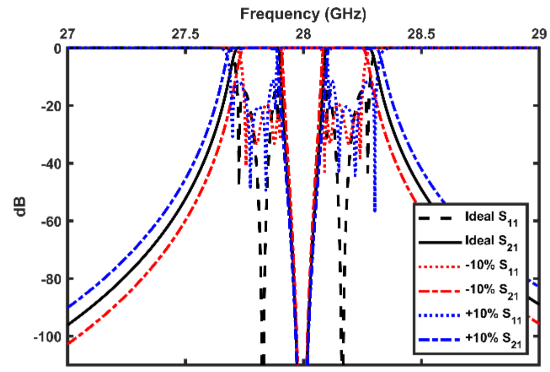

(j) S-parameter responses for twelfth-order chained-function filter

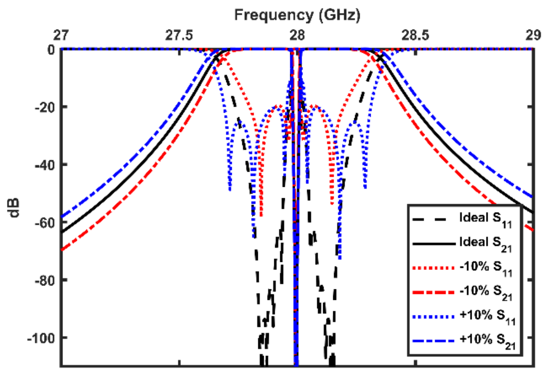

(k) S-parameter responses for twelfth-order conventional Chebyshev

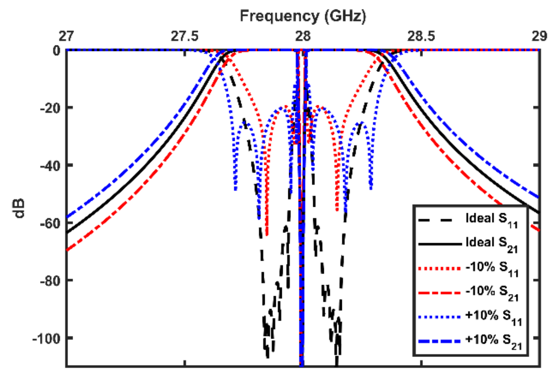

(l) S-parameter responses for twelfth-order Chebyshev of second kind

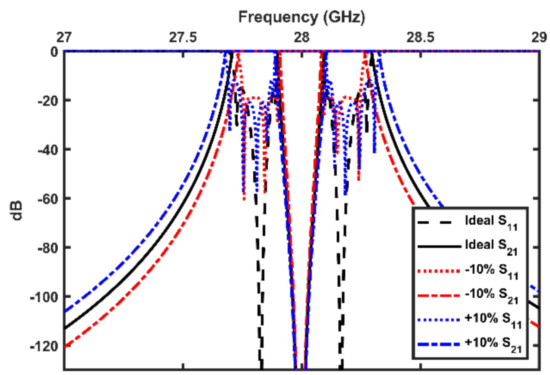

(m) S-parameter responses for fourteenth-order chained-function filter

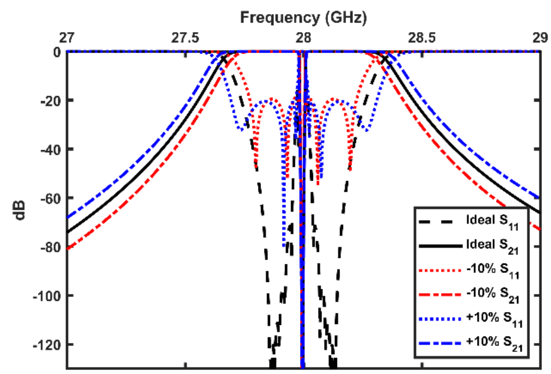

(n) S-parameter responses for fourteenth-order conventional Chebyshev

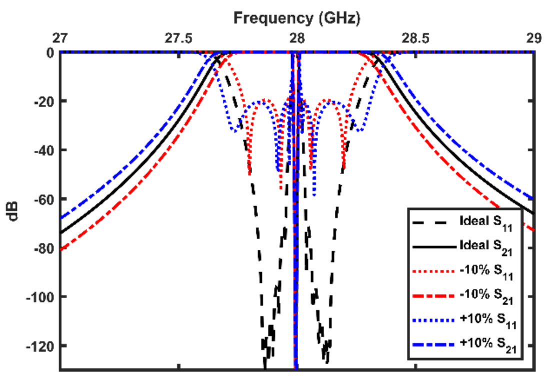

(o) S-parameter responses for fourteenth-order Chebyshev of second kind

FIGURE 13. ***(Continued.)*** **The effect of tolerance towards the S-parameter responses for chained-function, conventional Chebyshev, and Chebyshev of the second kind for filter order of six, eight, ten, twelve, and fourteen.**

TABLE 4. Comparison of return losses, insertion losses and bandwidths.

Class	Return Loss, RL (dB)			Insertion Loss, IL (dB)			Bandwidth			Percentage Change (%)					
										RL		IL		Bandwidth	
	Ideal	10%	-10%	Ideal	10%	-10%	Ideal	10%	-10%	10%	-10%	10%	-10%	10%	-10%
$C_6(\omega)$	15	19.04	11.84	1.1	0.7	1.59	840	865	800	26.93	21.07	36.36	44.55	2.98	4.76
$T_6(\omega)$	15	18.28	12.09	1.1	0.76	1.54	840	800	840	21.87	19.4	30.91	40	4.76	0
$U_6(\omega)$	15	18.34	12.07	1.1	0.76	1.54	840	800	840	22.27	19.53	30.91	40	4.76	0
$C_8(\omega)$	15	14.77	14.19	1.1	1.13	1.2	560	600	520	1.53	5.4	2.73	9.09	7.14	7.14
$T_8(\omega)$	15	14.33	14.56	1.1	1.18	1.15	560	600	530	4.47	2.93	7.27	4.55	7.14	5.36
$U_8(\omega)$	15	14.38	14.52	1.1	1.18	1.16	560	600	530	4.13	3.2	7.27	5.45	7.14	5.36
$C_{10}(\omega)$	15	12.4	18.31	1.1	1.48	0.76	560	620	500	17.33	22.07	34.55	30.91	10.71	10.71
$T_{10}(\omega)$	15	12.2	19.47	1.1	1.52	0.67	560	645	330	18.67	29.8	38.18	39.09	15.18	41.07
$U_{10}(\omega)$	15	12.2	18.55	1.1	1.52	0.74	560	645	390	18.67	23.67	38.18	32.73	15.18	30.36
$C_{12}(\omega)$	15	11.46	19.58	1.1	1.66	0.66	560	620	500	23.6	30.53	50.91	40	10.71	10.71
$T_{12}(\omega)$	15	11.46	19.61	1.1	1.66	0.66	560	665	400	23.6	30.73	50.91	40	18.75	28.57
$U_{12}(\omega)$	15	11.45	19.61	1.1	1.66	0.66	560	670	400	23.67	30.73	50.91	40	19.64	28.57
$C_{14}(\omega)$	15	11.84	18.8	1.1	1.59	0.72	560	620	500	21.07	25.33	44.55	34.55	10.71	10.71
$T_{14}(\omega)$	15	12.2	18.85	1.1	1.52	0.72	560	665	460	18.67	25.67	38.18	34.55	18.75	17.86
$U_{14}(\omega)$	15	11.84	18.88	1.1	1.59	0.71	560	670	460	21.07	25.87	44.55	35.45	19.64	17.86

TABLE 5. Rejection levels at 27.2 GHz and 28.8 GHz.

Class	Rejection Level (dB)					
	Ideal		10%		-10%	
	27.2 GHz	28.8 GHz	27.2 GHz	28.8 GHz	27.2 GHz	28.8 GHz
$C_6(\omega)$	22.39	19.67	18.62	15.84	26.55	23.93
$T_6(\omega)$	13.53	11.23	10.64	8.4	17.18	14.82
$U_6(\omega)$	13.46	11.06	10.48	8.261	17.09	14.61

TABLE 6. Rejection levels at 27.5 GHz and 28.5 GHz.

Class	Rejection Level (dB)					
	Ideal		10%		-10%	
	27.5 GHz	28.5 GHz	27.5 GHz	28.5 GHz	27.5 GHz	28.5 GHz
$C_8(\omega)$	31.42	29.19	26.46	24.13	36.82	34.69
$T_8(\omega)$	15.39	13.48	11.89	10.11	19.73	17.76
$U_8(\omega)$	15.27	13.38	11.56	10.03	19.6	17.64
$C_{10}(\omega)$	42.21	39.45	36.27	33.37	48.69	46.05
$T_{10}(\omega)$	19.46	17.13	15.38	13.13	24.39	22
$U_{10}(\omega)$	19.06	17.04	15.3	13.06	24.29	21.9
$C_{12}(\omega)$	52.45	49.15	45.58	42.14	59.96	56.8
$T_{12}(\omega)$	23.66	20.93	18.96	16.23	29.17	26.37
$U_{12}(\omega)$	23.59	20.85	18.89	16.17	29.08	26.29
$C_{14}(\omega)$	62.37	58.55	54.6	50.61	70.89	67.21
$T_{14}(\omega)$	28.04	24.91	22.58	19.38	34.16	30.99
$U_{14}(\omega)$	27.97	24.84	22.52	19.32	34.09	30.92

respectively, after applying −10% tolerance to its coupling matrices, while sixth- and fourteenth-order chained-function responses have 5.06% and 2.4% higher percentage changes of return loss, together with 5.45% and 6.37% higher percentage changes of insertion loss, respectively, after applying +10% tolerance to its coupling matrices.

In terms of comparisons of rejection levels shown in Table 5 and Table 6, chained-function responses of different orders, for a given maximum return loss level of 15 dB with cut-off frequencies at the stopbands, have an overall of higher rejection levels than the respective filter order responses of conventional Chebyshev and Chebyshev of the second kind. Therefore, it can be deduced that the overall implementation of the chained-function concept in a waveguide has the least amount of percentage changes for filter order of ten and above as compared with their respective performances of return loss, insertion loss, and total bandwidth.

However, the novel approach described in this paper is still applicable to sixth- and eighth-order chained-function filters, but with higher sensitivity to manufacturing errors. This proves the dual-band chained-function concept is a novel approach that can be exploited to extend the state-of-the-art in

TABLE 7. Comparison with previous works.

	[2]	[3]	[4]	[5]	[6]	[16]	[17]	**This work**
Band properties	Dual passbands							
Number of filters used	One	Two	One	Two	One			
Optimum and constant ripple	No, non-identical passband equal ripple	No		Yes		No		Yes
Return Loss (RL) flexibility	No, depend on iteration procedures	No, depend on approximation methods		Yes, using Chebyshev RL formulas		No, depend on semi-lumped based on CRLH line	No, depend on Remez-Like algorithm	Yes, using Chained RL formula
Adjacent Band' rejection at f_0 (High = ≥ 100dB)	Low	High	Low					High
No bandwidth increasing for high filter order	No							Yes

tuning-less high-performance filter implementations towards higher frequencies and narrowband applications.

V. COMPARISON WITH PREVIOUS WORKS

Table 7 shows a comparison of previous works with the method proposed in this paper. For comparison, the method of chaining second kind Chebyshev polynomials proposed in this paper gains the advantage of having a smaller number of filters used than the methods listed in [3], [5]. This is essential for narrowband filter designs as the more filters involved will contribute to a higher filter loss. This method is also able to produce an optimum and constant ripple if compared to the approaches listed in [2]–[4], [16], [17], as the constant ripple ensures the filters to have minimum insertion loss. In addition, this method is able to support filter orders greater than five without increasing the bandwidth, rather than enlarging the bandwidths listed in [2]–[6], [16], [17] for the narrowband applications. This is because the proposed method will always produce a constant number of six distinct reflection poles for the higher filter orders, instead of having many reflection poles distributed over an extremely small frequency range, leading to time-consuming simulations and fabrication issues.

To add on, the adjacent bands' rejection at f_0 of this method is also higher if compared to [2], [4]–[6], [16], [17] due to having multiple transmission zeros placed at the centre frequency. Higher adjacent bands' rejection ensures that two bands will not interfere with each other and thus, eliminating the unwanted signals efficiently. This is vital for the application of the Internet of Things (IoT) which has proximity bands that cause multichannel interferences.

Besides that, the proposed method allows flexibility in return loss using the generalised ripple factor of chained function derived in (16). This is able to achieve identical passband equal ripple if compared to the methods mentioned in [2]–[4], [16], [17], which use methods that possess non-identical passband equal ripple. Not to mention, the respective number of TZs for different filter orders can also be calculated to achieve dual-band filters with passband equal ripple.

VI. CONCLUSION

This paper presented for the first time a method of synthesis involving uncommon Chebyshev of the second kind that has passband unequal ripple, and realize it as an equal-ripple dual-band filter by introducing transmission zeros at the centre frequency to the chained Chebyshev of the second kind. The method is flexible, is not restricted to certain filter types or topologies, and is capable of being implemented for higher filter orders.

The advantages of this proposed technique are the characteristics of optimum and constant ripple, the flexibility of return loss, and the high adjacent bands' rejection. The proposed technique has been realised to the sixth-order dual-band waveguide filter with a prescribed return loss of 15 dB centred at a frequency of 28 GHz and a total bandwidth of 840 MHz. The measured responses show that the return loss, bandwidth, and the frequency shift are 12 dB, 860 MHz, and 0.24%, respectively. By referring to the filter sensitivity tests, in order to have a lower discrepancy of frequency shift, filter order greater than nine is considered as the number of distinct reflection poles will always be a constant at six, due to the seed function characteristics of chained functions. The proposed synthesis approach is limited to symmetrical dual-band filter designs with identical passband equal ripple. In fact, it is possible to realise asymmetrical dual-band filter designs by adjusting the position of the transmission zeros. However, identical passband equal ripple will not be achieved which lead to a higher filter loss in either band.

The feasibility of this technique is demonstrated for filter configurations in waveguide technology. The sixth-order dual-band filter design is verified by measurements. This technique can be applied to realize multi-band filters by introducing transmission zeros at different locations in the future.

REFERENCES

[1] S. Bila, R. Cameron, P. Lenoir, V. Lunot, and F. Seyfert, "Chebyshev synthesis for multi-band microwave filters," in *IEEE MTT-S Int. Microw. Symp. Dig.*, Nov. 2006, pp. 1221–1224.
[2] Y. Zhang, K. A. Zaki, J. A. R. Cruz, and A. E. Atia, "Analytical synthesis of generalized multi-band microwave filters," in *IEEE MTT-S Int. Microw. Symp. Dig.*, Jul. 2007, pp. 1273–1276.
[3] L. C. Tsai and C. W. Hsue, "Dual-band bandpass filters using equal-length coupled-serial-shunted lines and Z-transform technique," *IEEE Trans. Microw. Theory Techn.*, vol. 52, no. 4, pp. 1111–1117, Apr. 2004.
[4] H. M. Lee, C. R. Chen, C. C. Tsai, and C. M. Tsai, "Dual-band coupling and feed structure for microstrip filter design," in *IEEE MTT-S Int. Microw. Symp. Dig.*, Fort Worth, TX, USA, Oct. 2004, pp. 1971–1974.
[5] G. Macchiarella and S. Tamiazzo, "Dual-band filters for base station multi-band combiners," in *IEEE MTT-S Int. Microw. Symp. Dig.*, Honolulu, HI, USA, Jun. 2007, pp. 1289–1292.
[6] X.-P. Chen, K. Wu, and Z.-L. Li, "Dual-band and triple-band substrate integrated waveguide filters with Chebyshev and quasi-elliptic responses," *IEEE Trans. Microw. Theory Techn.*, vol. 55, no. 12, pp. 2569–2578, Dec. 2007.
[7] P. Lenoir, S. Bila, F. Seyfert, D. Baillargeat, and S. Verdeyme, "Synthesis and design of asymmetrical dual-band bandpass filters based on equivalent network simplification," *IEEE Trans. Microw. Theory Techn.*, vol. 54, no. 7, pp. 3090–3097, Jul. 2006.
[8] G. Macchiarella and S. Tamiazzo, "Design techniques for dual-passband filters," *IEEE Trans. Microw. Theory Techn.*, vol. 53, no. 11, pp. 3265–3271, Nov. 2005.
[9] R. Cameron, "General coupling matrix synthesis methods for Chebyshev filtering functions," *IEEE Trans. Microw. Theory Techn.*, vol. 47, no. 4, pp. 433–442, Apr. 1999.
[10] C. Chrisostomidis and S. Lucyszyn, "On the theory of chained-function filters," *IEEE Trans. Microw. Theory Techn.*, vol. 53, no. 10, pp. 3142–3151, Oct. 2005.
[11] C. Chrisostomidis and S. Lucyszyn, "Seed function combination selection for chained function filters," *IET Microw. Antennas Propag.*, vol. 4, no. 6, pp. 799–807, Jun. 2010.
[12] C. E. Chrisostomidis, M. Guglielmi, P. Young, and S. Lucyszyn, "Application of chained functions to low-cost microwave band-pass filters using standard PCB etching techniques," in *Proc. 30th Eur. Microw. Conf.*, Paris, France, Oct. 2000, pp. 1–4.
[13] R. J. Cameron, C. M. Kudsia, and R. R. Mansour, *Microwave Filters for Communication Systems: Fundamentals, Design, and Applications*, 2nd ed. New York, NY, USA: Wiley, 2018.
[14] Y. P. Lim, Y. L. Toh, S. Cheab, G. S. Ng, and P. W. Wong, "Chained-function waveguide filter for 5G and beyond," in *Proc. IEEE Region 10 Conf. (TENCON)*, Jeju, Korea, Oct. 2018, pp. 107–110.
[15] Y. P. Lim, Y. L. Toh, S. Cheab, S. Lucyszyn, and P. W. Wong, "Coupling matrix synthesis and design of a chained-function waveguide filter," in *Proc. Asia–Pacific Microw. Conf. (APMC)*, Kyoto, Japan, Nov. 2018, pp. 103–105.
[16] M. D. Sindreu, J. Bonache, and F. Martin, "Compact CPW dual-band bandpass filters based on semi-lumped elements and metamaterial concepts," in *Proc. Asia–Pacific Microw. Conf.*, Yokohama, Japan, Dec. 2010, pp. 670–673.
[17] G. Macchiarella, "'Equi-ripple' synthesis multiband prototype filters using a Remez-like algorithm," *IEEE Microw. Wireless Compon. Lett.*, vol. 23, no. 5, pp. 231–233, May 2013.

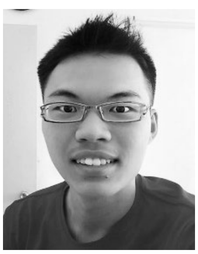

YUHAO LEONG received the B.Eng. (Hons.) degree in electrical and electronics engineering from the Petronas University of Technology, Perak, Malaysia, in 2017, where he is currently pursuing the M.Sc. degree in microwave engineering.

His current research interest includes the design and synthesis of multiband microwave filters and millimeter-wave waveguide filters. He received the Petronas University of Technology Scholarship of electrical and electronics engineering.

SOVUTHY CHEAB (Member, IEEE) was born in Battambang, Cambodia. He received the B.Eng. (Hons.) degree in electrical and electronic engineering, and the M.Sc. and Ph.D. degrees in microwave engineering from the Petronas University of Technology, Perak, Malaysia, in 2010, 2012, and 2015, respectively.

During the Ph.D. degree from the Petronas University of Technology, he was also involved in many communication system design projects including the design of a RFID RF front end system. He currently works as a Lecturer with the Petronas University of Technology, where he is teaching electromagnetic theory and communication system courses. His research interest includes the design and synthesis of microwave filters involving multimode and multiband filters in both planar and cavity realisations. He serves as a Reviewer for *Progress in Electromagnetics Research* (PIER). He is currently a member of the MTTS and a Committee Member of the IEEE ED/MTT/SSC, Penang Chapter, Malaysia.

SOCHEATRA SOEUNG (Member, IEEE) was born in Phnom Penh, Cambodia, in 1986. He received the B.Eng. (Hons.) degree in electrical and electronic engineering, majored in computer system architecture, the M.Sc. degree by research on PCB testing based on Eddy current, and the Ph.D. degree by research in RF microwave engineering from the Petronas University of Technology, Perak, Malaysia, in 2010, 2013, and 2018, respectively.

He worked as a Research Officer under project Wireless Communication Using Evaporation Duct (WiDuct) with the responsibility to RF frontend design, implementation, and testing. He is currently a member of the MTT and a Committee Member of the IEEE ED/MTT/SSC Penang Chapter, Malaysia, and the IEEE Consultants Network Affinity Group, Malaysia. He currently works as a Lecturer with the Electrical and Electronic Engineering Department, Petronas University of Technology. His research interests include lossy filter, passive microwave filter, and multiband filter design techniques.

PENG WEN WONG (Senior Member, IEEE) received the B.Eng. degree (Hons.) in electrical and electronic engineering from the University of Leeds, in 2005, and the Ph.D. degree from the University of Leeds, U.K., in 2009.

During the Ph.D. degree, he was involved in a U.K. DTI-funded project developing process design kits for multilayer system-in-package modules. He was fully funded by the U.K. Ministry of Defense through the DTC Program. He currently works as an Associate Professor with the Petronas University of Technology, Perak, Malaysia. His research interests include reconfigurable filters, the design of lossy filters, millimeter-wave waveguide filters, and passive filter miniaturisation techniques.

Dr. Wong is also an Associate Fellow of the AAET. He has served as an invited speaker locally and internationally including at APMC 2017 and a keynote speaker at ICCSP 2017. He is currently an Advisor of the IEEE Penang Joint Chapter. He has received the Outstanding Researcher Award, in 2013, a publication award, in 2014, and the Potential Academy Award of the Year, in 2015. He received the Switched Reluctance Drive Award of electrical and electronics engineering. He has served as the Technical Chair for IMESS 2017 and 2018. He was the Former Chair of the IEEE ED/MTT/SSC Penang Chapter, from 2016 to 2017. He was the Founding Chair of the IEEE International Microwave, Electron Devices, and Solid-State Symposium (IMESS), in 2016. He serves as a Reviewer for the IEEE Transactions on Microwave Theory and Techniques, the IEEE Microwave and Wireless Components Letters, *IET Microwaves, Antennas & Propagation*, and *PIERS*.